ISSN: 0067-2904

Gamma-Ray Shielding Effectiveness of Clay and Boron Doped Clay Material at Different Thicknesses

Akram Mohammed Ali *, Ahmed Salih Sameer
Physics Department, College of Science, University of Anbar, Al-Anbar, Iraq

Received: 10/9/2020 Accepted: 1/8/2021 Published: 30/5/2022

Abstract

In this work, the gamma-ray shielding parameters of red clay and boron-doped red clay with different sample thicknesses are theoretically and experimentally reported. These shielding parameters are considered at a photon energy of 0.662 MeV emitted from ^{137}Cs. The theoretical calculations are demonstrated using the XCom software program, while a scintillation detector, NaI(TI), with an efficiency of 98% is used to attain the experimental results of the mass attenuation coefficient of the prepared samples. The acquired results show that the boron-doped clay delivers a higher mass attenuation coefficient as compared to those of pure clay. Additionally, the mass attenuation coefficient exhibits an increasing behavior with the sample thickness increment.

Keywords: red clay, mass attenuation coefficient, gamma-ray, Boron, scintillation detector.

فاعلية التدريع لأشعة جاما لمادة الطين والطين المشوب بالبورون عند سماكات مختلفة

أكرم محمد علي*، أحمد صالح سمير
قسم الفزياء، كلية العلوم، جامعة الانبار، الانبار، العراق

الخلاصة

في هذا البحث، معلمات التدريع لأشعة غاما للطين الأحمر والطين الأحمر المشوب بالبورون تم دراستها نظريا وعملياً مع الأخذ في الاعتبار سماكات مختلفة للعينات. معلمات التدريع تم حسابها عند طاقة الفوتون البالغة 0.662 ميجا فولت المنبعثة من مصدر السيزيوم-137. تم عرض الحسابات النظرية باستخدام برنامج XCom ، بينما تم استخدام كاشف الوميضي(TI) NaI بكفاءة 98٪ لتحقيق النتائج التجريبية لمعامل التوهين الكتلي للعينات المحضرة. أظهرت النتائج أن عينات الطين المشوب بالبورون أعطت معامل توهين كتلي أعلى مقارنة بتلك الخاصة بالطين النقي. بالإضافة إلى ذلك ، أظهر معامل التوهين الكتلي سلوكًا متزايدًا مع زيادة سماكة العينات.

1. Introduction

Gamma emitting radioisotopes are widely used in several applications such as in medicine, agriculture, and industry [1]. It is a well-established fact that gamma-rays are a type of electromagnetic radiation that are transmitted in a distance of miles in a second. Hence, it is of crucial importance to form shielding materials for blocking this specific type of radiation. Concrete and lead are commonly used as gamma radiation shields. However, concrete and

*Email: dr.akram@uoanbar.edu.iq

lead are assumed as unsuitable materials for this purpose due to: (1) lack of transparency, (2) difficulty in transportation, (3) cracks formation after a long period of nuclear radiation exposure, (4) high cost and toxicity, and (5) alteration in the cement water content at relatively high gamma-rays energy [1, 2]. Interestingly, among many proposed materials to overcome the addressed issue, clay is well-thought-out as an applicable shielding material. Such a consideration is mainly attributed to the fascinating clay features such as cost-effectiveness, non-poisonous, and eco-friendly [3]. Radiation shielding properties in clays can be used to investigation the photon attenuation coefficients of clay produced using different rate of boron.

Many studies deal with the different type of materials, for example, concrete and other building materials that are used for shielding of gamma-ray [4]. Other studies have aimed at calculating the mass attenuation coefficients of different construction materials, such as ceramic and clay-fly ash, in order to evaluate their gamma ray attenuation abilities [5,6,7]. The shielding efficiency of boron-doped clay was reported by Akkurt and Canakci [8]. They measured the linear attenuation coefficient of clay of different boron content and found an increase in the linear attenuation coefficient with boron percentage increment in clay.

This study reports an experimental and theoretical examination of red clay materials for gamma-ray attenuation at a photon energy of 0.662 MeV discharged from ^{137}Cs. Boron was added to the employed clay in which the enhancement of shielding parameters was systematically estimated. Additionally, the effect of clay thickness was experimentally investigated.

2. Theory

Following Lambert-Beer law, a mono-energetic gamma beam can be attenuated as given in the following formula [7, 8]:

$$I=B\, I_o e^{-(\mu/\rho)\,\rho\, t} \quad (1)$$

Where B is the build-up factor. The incident and transmitted photon intensity are represented by I_o and I, respectively. While, the symbols ρ, t are the density and thickness of the sample, respectively. The term μ/ρ signifies the mass attenuation coefficient(μ_s). The (μ_s) for compound and/or mixture is expressed by Equation (2) [5]:

$$\mu_s = \sum \omega_i (\mu_s)_i \quad (2)$$

where: ω_i refers to the weight fraction and $(\mu_s)_i$ is the mass attenuation coefficient of the i^{th} element; where $\omega_i = a_i A_i / \sum a_i A_i$.

The effective atomic number (Z_{eff}) of any mixture and/or compound can be calculated by [1,9, 10,11]:

$$Z_{eff} = \sigma_a/\sigma_e \quad (3)$$

where σ_a and σ_e are the atomic and electronic cross sections, respectively. These quantities can be attained by the equations [10,11]:

$$\sigma_a = \frac{1}{N_A}\sum_i f_i A_i (\mu_s)_i \quad (4)$$

$$\sigma_e = \frac{1}{N_A}\sum_i \frac{f_i}{Z_i} A_i (\mu_s)_i \quad (5)$$

Where N_A is Avogadro's constant, f_i, is the element i fractional abundance, while A_i, and Z_i are the constituent element atomic number and atomic weight, respectively.

Finally, the effective electron density (N_e) is expressed as [10,12]:

$$N_{eff} = \left(\frac{Z_{eff}}{M}\right) N_A \sum_i n_i \quad (6)$$

The mean free path (MFP), and half-value layer (HVL) are crucial factors for determining the average distance between two interactions and are measured by the equations [4,13]:

$$MFP = \frac{1}{\mu} \quad (7)$$

$$HVL = \frac{ln2}{\mu} \quad (8)$$

3. Methodology

3.1 Preparation of Undoped and Boron Doped Clay Materials

The utilized red clay material was obtained from Al-Rutbah (33°N 40°E) at the west of Al-Anbar governorate in Iraq. The collected clay was crushed to a certain size and later dried naturally according to ASTM recommendations [9]. Continuously, the crushed material was pulverized, filtered (with 2 μm mesh size), and consequently pelletized. Three sets denoted as R1, R2, and R3 were accordingly molded. Each set is composed of three circular-shaped samples with a fixed radius of 3cm but of different thicknesses (0.5, 1, and 2 cm). R1 refers to pure clay (with the chemical formula $Al_2H_6O_{10}Si_2$), R2 to pure clay baked at 1000 °C, and R3 to pure clay doped with 2% boron (with the chemical formula $Al_2H_6O_{10}Si_2B_5$) and later baked at 1000 °C for 1 hour (Figure 1).

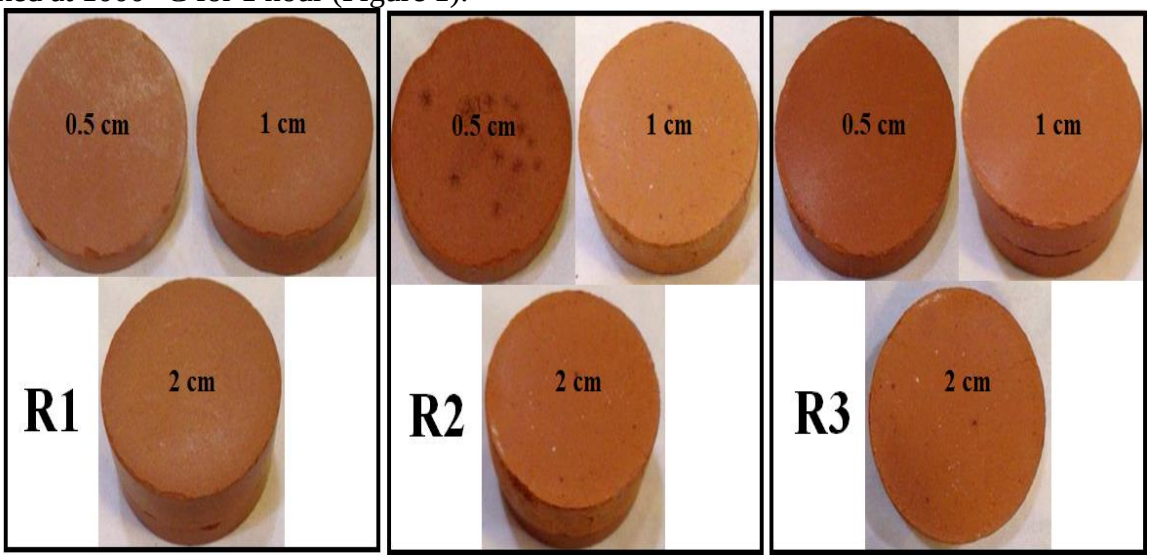

Figure 1-Molded samples of different thicknesses (0.5, 1, and 2 cm).

3.2 Measurement Setup

The experimental investigations of the linear attenuation coefficient for the proposed samples (R1, R2, and R3) were accomplished using gamma-rays at a photon energy of 0.662 MeV emitted from ^{137}Cs point source ($T_{1/2} = 30\ year$). Figure 2 displays the measurement setup used in this study. The pelletized samples were positioned between the gamma source and NaI(TI) detector at a 1cm distance from the face of the detector**.** Thereby the data was collected on Integrated Computer Spectrometer (PCI-ICS card) linked to a personal computer.

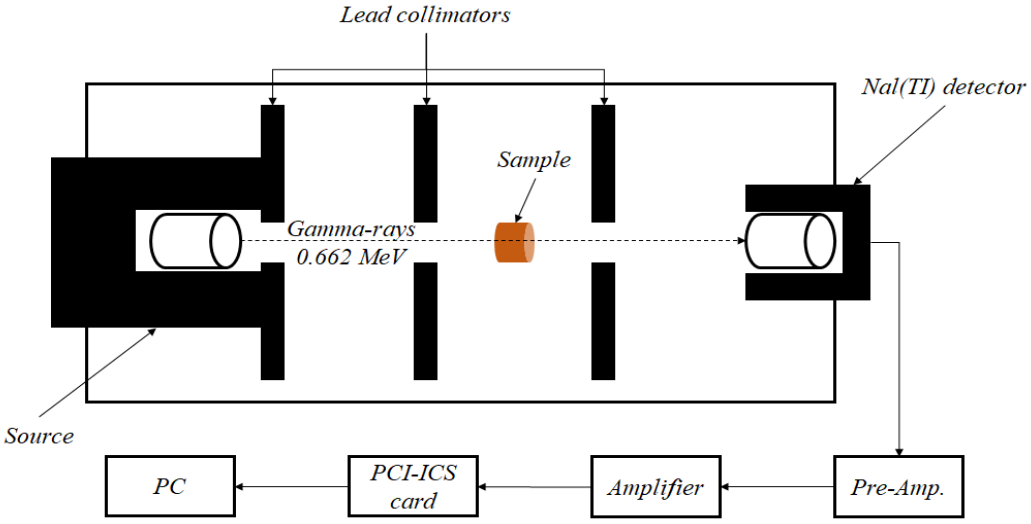

Figure 2-Schematic illustration of the measurement setup.

4. Results and Discussion

4.1 Theoretical Results Using XCom

The theoretical shielding quantities (i.e. μ/σ) by which the pelletized clay samples' gamma radiation shielding capability are to be evaluated were performed on XCom software. The obtained results are demonstrated in Table 1.

Table 1-Mass scattering coefficient (Compton scattering) theoretical values of the compounds using Win XCom software at the energy of 0.662 MeV.

Compound	μ_s $(cm^2 g^{-1})$	$\sigma_{t,a}$ (barn/atom)	$\sigma_{t,e}$ (barn/atom)	Z_{eff}	$N_{el}x10^{23}$ (electrons/g)
SiO_2	0.0773	2.570	0.257	10.000	3.01
Si	0.0361		0.040		
O	0.0412		0.091		
Al_2O_3	0.0759	2.569	0.257	10.000	2.95
Al	0.0402		0.055		
O	0.0357		0.071		
Fe_2O_3	0.0746	3.956	0.260	15.200	2.87
Fe	0.0522		0.074		
O	0.0224		0.045		
Na_2O	0.0749	2.568	0.256	10.024	2.92
Na	0.0555		0.128		
O	0.0193		0.021		
K_2O	0.0760	3.962	0.258	15.333	2.94
K	0.0631		0.144		
O	0.0129		0.014		
Ca_2CO_3	0.0776	3.010	0.258	11.667	3.01
Ca	0.0444		0.049		
C	0.0066		0.004		
O	0.0266		0.044		
MgO	0.0768	2.569	0.257	10.000	2.99
Mg	0.0463		0.078		
O	0.0305		0.051		
TiO	0.0733	3.884	0.259	15.000	2.83
Ti	0.0549		0.099		
O	0.0183		0.030		
B	0.0714	1.280	0.256	5.000	2.79

Figure 3 presents different compounds' theoretical (μ_s) values acquired via XCom software using an energy range from 0.1 to 1 MeV. it can be observed from the figure that the attained (μ_s) decreases with the increment of the applied energy. The value of (μ_s) different compounds at a photon energy of 0.662 MeV is also demonstrated.
Furthermore, the utilized chemical formula of this experimental work regarding red clay and boron-doped red clay was also investigated and subsequently elaborated in Table 2 using XCom software; thereby the shielding parameters such as (μ_s), σ_a, σ_e, Z_{eff}, and N_e are presented. It should be mentioned that the attained theoretical values are in an upright agreement with those obtained experimentally.

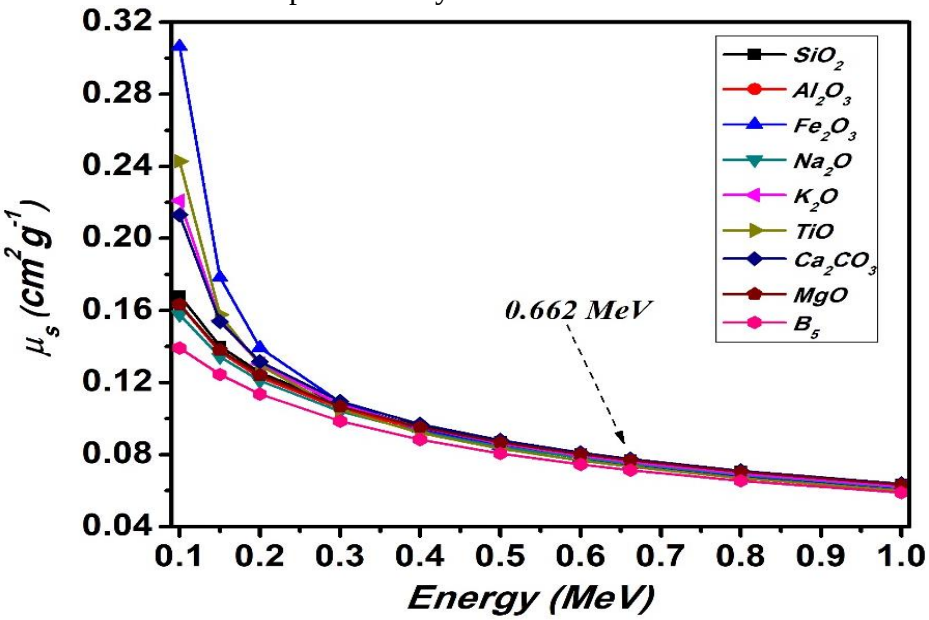

Figure 3- Mass attenuation coefficient as a function of energy for clay compounds after the chemical analysis.

Table 2-Theoretical values of both clay and boron-doped clay with chemical formulas $Al_2H_6O_{10}Si_2$ and $Al_2H_6O_{10}Si_2B_5$, respectively.

Sample	μ_s (cm^2g^{-1})	σ_a **(barn/atom)**	σ_e **(barn/atom)**	Z_{eff}	$N_{el}x10^{23}$ **(electrons/g)**
$Al_2H_6O_{10}Si_2$	0.0784	1.9775	0.2152	9.190	3.64
Al	0.0153		0.0318		
H	0.0011		0.0309		
O	0.0409		0.1379		
Si	0.0160		0.0307		
Sample	μ_s (cm^2g^{-1})	σ_a **(barn/atom)**	σ_e **(barn/atom)**	Z_{eff}	$N_{el}x10^{23}$ **(electrons/g)**
$Al_2H_6O_{10}Si_2B_5$	0.0773	1.8209	0.0714	25.519	1.08
Al	0.0134		0.0242		
H	0.0010		0.0235		
O	0.0356		0.1050		
Si	0.0139		0.0234		
B	0.0134		0.0631		

4.2 Results and discussions:

The red clay material employed in this work has the compositions listed in Table 3.

Table 3- Red clay material chemical composition by weight %

Materials composition	%	Mineralogy
SiO_2	45.50	Kaolinite
Al_2O_3	24.40	Illite
Fe_2O_3	7.85	Smectite
Na_2O	0.78	Quartz
K_2O	1.12	Goethite
TiO	1.33	Anatas
Ca_2CO_3	5.65	Halite
MgO	1.68	Kaolinite
Loss of ignition	12.00	Illite

Figure 4 demonstrates the variation of the measured $\ln(\frac{I_o}{I})$ with the thickness of the clay samples. It can be noticed that, generally, all the samples exhibited an increasing behavior $\ln(\frac{I_o}{I})$as the thickness increased from 0.5 to 2 cm. However, this was not the case for sample R3, whereby the prepared R3 samples exhibited a decreased profile at a thickness of 1 cm and subsequently increased to a value above 0.3 when the thickness was 2 cm. The reason for this result may be because the necessary preparation conditions for the sample under study such as humidity, high pressure or temperature, were not considered which led to the formation of crack in the resulting sample. The general behavior shows a linearity dependence between the thickness of the sample and the measured $\ln(\frac{I_o}{I})$.

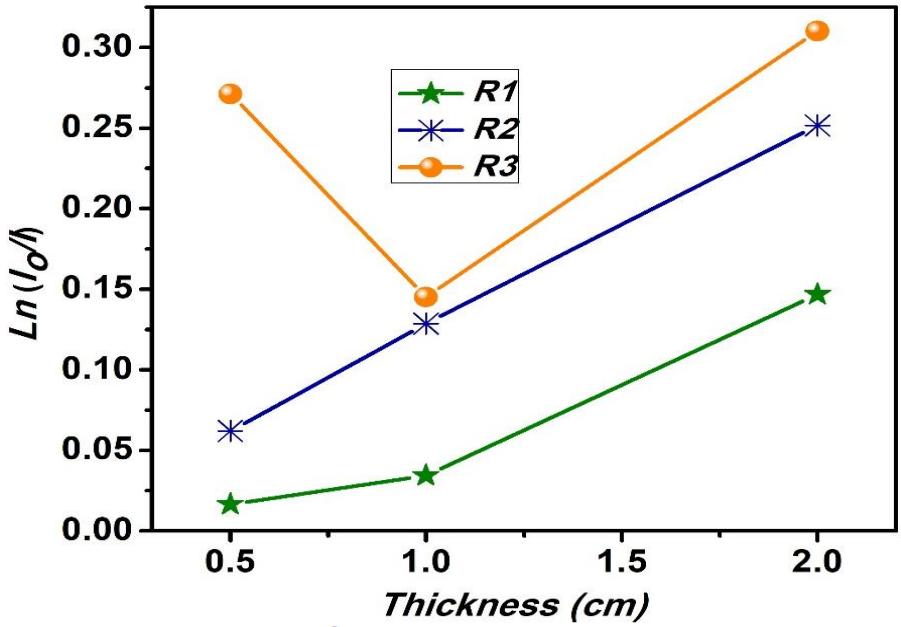

Figure 4- The measured $\ln(\frac{I_o}{I})$ as a function of the thickness of the samples.

Figure 5 (a) shows the linear attenuation coefficient as a function of the sample thickness for R1, R2, and R3. For R1, there was a slight increase in the value of μ, while for R2 the values were constant but R3 revealed a decrease in the measured linear attenuation coefficient but increased after 1cm. This behavior is attributed to the fact that the correlation between the linear attenuation coefficient and the utilized thickness is inversely proportional according to the relation [$I = I_o \exp(-\mu x)$].

In the figure (5-b), linear attenuation coefficients for the sets R1, R2, and R3 at a thickness of 0.5 cm shows that the addition of boron at a percentage of 2 % has given the highest linear attenuation coefficient.

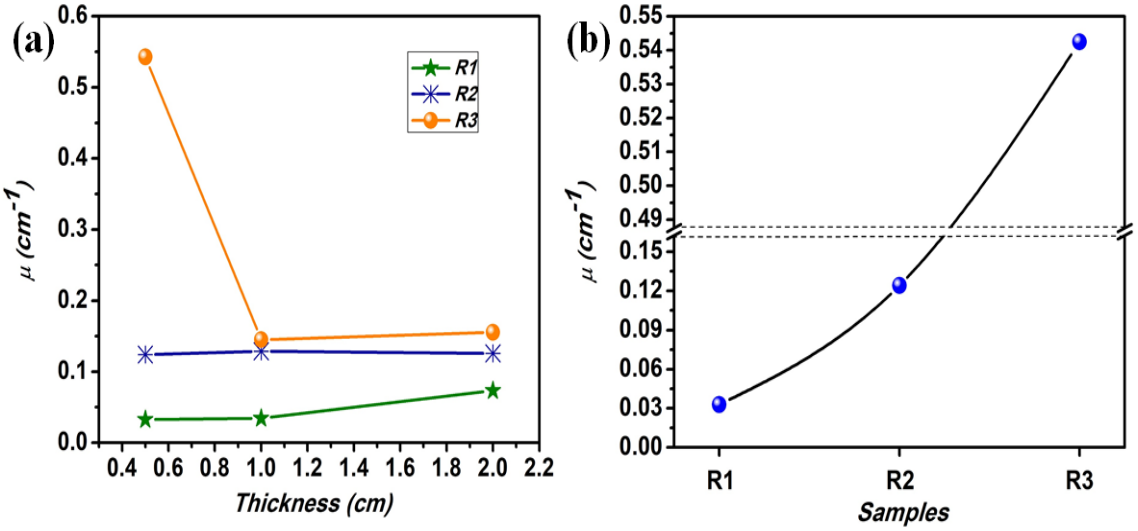

Figure 5- (a) linear attenuation coefficient values versus thickness, (b) linear attenuation coefficient for the three sets at a thickness of 0.5 cm; section-break feature is applied from 0.16 to 0.48 cm^{-1}.

Figure 6 illustrates the experimentally obtained mass attenuation coefficient (μ_s) against the thickness of the prepared samples. It is noticed, from the figure, that the obtained (μ_s) values increased, for the samples of pure clay baked at 1000 °C, with the increase of thickness, and further increased when doped with boron. Additionally, increasing the sample thickness(for R1 and R2) resulted in generally higher values of the experimentally attained (μ_s). However, in the case of boron-doped clay (R3), a noticeable decrease in the values (μ_s) was noticed when the thickness decreased from 0.5 to 1 cm. Moreover, the samples doped with boron showed higher values of the calculated (μ_s) since the density was increased when boron was added. This demonstrates the effect of boron on the shielding capability of the utilized clay material [4, 10, 11]. In comparison with other results, our findings demonstrated higher (μ_s) upon baking the sample [12]. The results are demonstrated in detail in Tables (4, 5, and 6) for R1, R2, and R3, respectively.

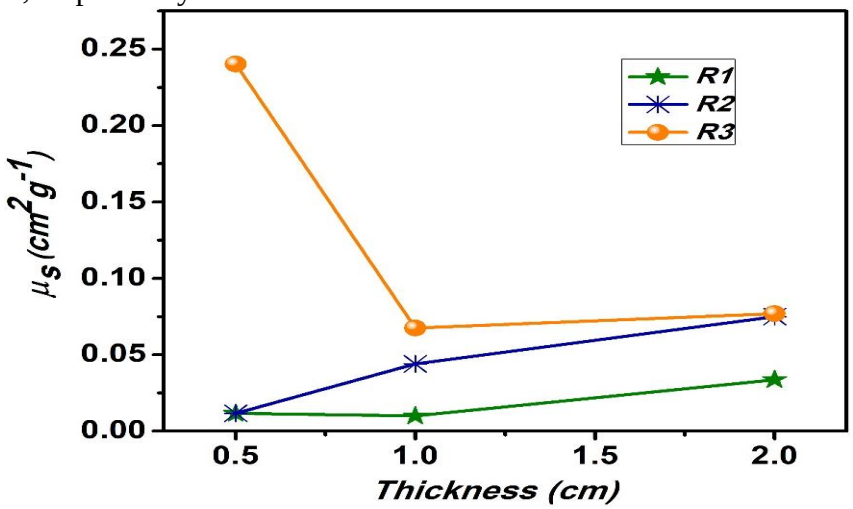

Figure 6- Experimentally obtained (μ_s) values with the thickness of the prepared samples R1, R2, and R3.

Figure 7 displays the HVL (calculated from Eq.8) and MFP (calculated from Eq.7) of the prepared R1, R2, and R3 against the applied linear attenuation coefficients of each sample. Both the HVL and the MFP decreased with the increment of the sample linear attenuation coefficient. Moreover, generally, the MFP and HVL values were found to be decreased in the perspective of the state of treatment; this can be clearly stated as the HVL and MFP for R3>R2>R1.

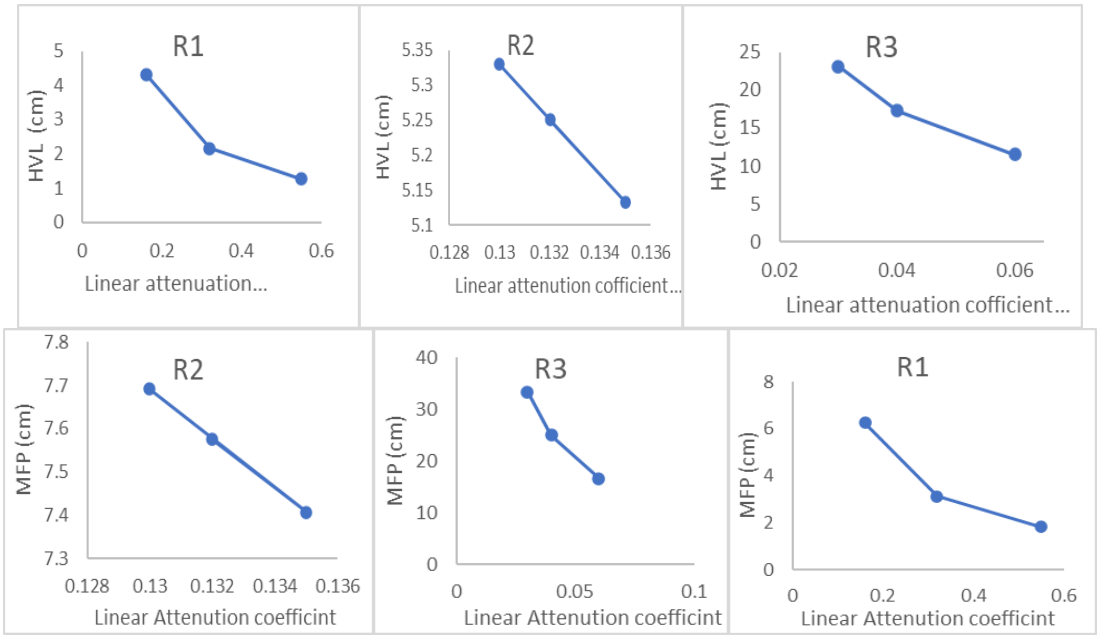

Figure 7-The evaluated HVL and MFP for the prepared R1, R2, and R3 as a function of linear attenuation coefficient.

The σ_a, σ_e, Z_{eff}, and N_e values for the prepared samples (R1, R2, and R3) are demonstrated in Tables 4, 5, and 6, respectively. These values were calculated based on the experimentally obtained (μ_s) using equation (3) through equation (6). In Tables 4 and 6, the values of Z_{eff}, and $N_e$in R1 and R2 are similar which can be because the mentioned values depend directly on the experimentally acquired (μ_s); the (μ_s) values for R1 and R2 are quite similar. However, sample R3 (boron-doped clay) showed noticeably higher values in terms of Z_{eff}, and N_e as compared to R1 and R2, since these samples have higher (μ_s) than that of R1 and R2. Comparing these results with those in Table 1, one can be concluded that the experimental mass attenuation coefficients are less than the theoretical values because of the theoretical take into account the three types of scattering (photoelectric effect, Compton, and pair production).

Table 4-Experimental values of (μ_s), σ_a, σ_e, Z_{eff}, and N_e for R1.

compound/ element	$\sum w(i)$	μ_s *(cm²/g)*	σ_a *(barn/atom)*	σ_e *(barn/atom)*	Z_{eff}	$N_e x10^{23}$ *(electrons/g)*
The thickness of 0.5 cm						
$Al_2H_6O_{10}Si_2$	-	0.0116	0.2663	0.0317	8.412	3.67
Al	0.195	0.0023		0.0040		
H	0.022	0.0003		0.0058		
O	0.579	0.0067		0.0193		
Si	0.203	0.0024		0.0039		
The thickness of 1cm						
$Al_2H_6O_{10}Si_2$	-	0.0100	0.2284	0.0271	8.412	3.67
Al	0.195	0.0019		0.0034		
H	0.022	0.0002		0.0050		

O	0.579	0.0058		0.0165		
Si	0.203	0.0020		0.0033		
The thickness of 2cm						
$Al_2H_6O_{10}Si_2$	-	0.0684	0.7715	0.0917	8.412	3.67
Al	0.195	0.0143		0.0116		
H	0.022	0.0011		0.0169		
O	0.579	0.0381		0.0559		
Si	0.203	0.0149		0.0112		

Table 5- Experimental values of (μ_s), σ_a, σ_e, Z_{eff}, and N_e for R2.

compound/ element		μ_s ***(cm²/g)***	σ_a ***(barn/atom)***	σ_e ***(barn/atom)***	Z_{eff}	$N_e x10^{23}$ ***(electrons/g)***
Thickness of 0.5cm						
$Al_2H_6O_{10}Si_2$	-	0.0345	0.7917	0.0941	8.412	3.67
Al	0.195	0.0067		0.0119		
H	0.022	0.0008		0.0173		
O	0.579	0.0200		0.0573		
Si	0.203	0.0070		0.0115		
The thickness of 1cm						
$Al_2H_6O_{10}Si_2$		0.0440	1.0084	0.1199	8.412	3.67
Al	0.195	0.0086		0.0152		
H	0.022	0.0010		0.0221		
O	0.579	0.0255		0.0730		
Si	0.203	0.0089		0.0146		
The thickness of 2cm						
$Al_2H_6O_{10}Si_2$	-	0.0750	1.7186	0.2043	8.412	3.67
Al	0.195	0.0146		0.0258		
H	0.022	0.0016		0.0376		
O	0.579	0.0434		0.1245		
Si	0.203	0.0152		0.0250		

Table 6- Experimental values of (μ_s), σ_a, σ_e, Z_{eff}, and N_e for R3.

compound/ element		μ_s ***(cm²/g)***	σ_a ***(barn/atom)***	σ_e ***(barn/atom)***	Z_{eff}	$N_e x10^{23}$ ***(electrons/g)***
The thickness of 0.5 cm						
$Al_2H_6O_{10}Si_2B_5$	-	0.2403	5.2701	0.2205	23.905	1.09
Al	0.163	0.0393		0.0662		
H	0.018	0.0044		0.0965		
O	0.484	0.1164		0.3192		
Si	0.170	0.0409		0.0640		
B	0.164	0.0393		0.1725		
The thickness of 1 cm						
$Al_2H_6O_{10}Si_2B_5$	-	0.0674	1.4784	0.0618	23.905	1.09
Al	0.163	0.0110		0.0186		
H	0.018	0.0012		0.0271		
O	0.484	0.0327		0.0895		
Si	0.170	0.0115		0.0180		
B	0.164	0.0110		0.0484		
The thickness of 2 cm						
$Al_2H_6O_{10}Si_2B_5$	-	0.0770	1.6880	0.0706	23.905	1.09
Al	0.163	0.0126		0.0212		
H	0.018	0.0014		0.0309		
O	0.484	0.0373		0.1022		
Si	0.170	0.0131		0.0205		
B	0.164	0.0126		0.0553		

Conclusion

Red clay and boron-doped clay as gamma-ray shielding materials were successfully introduced and investigated. The shielding parameters such as (μ_s), HVL, MFP, Z_{eff}, and N_e were experimentally and theoretically attained at 0.662 photon energy. The obtained results showed that the R3 samples (boron-doped clay) have larger (μ_s) in comparison to the clay treated at both room temperature and 1000 °C. Furthermore, it can be generally stated that the higher thickness of the samples resulted in higher shielding parameters. Finally, the established effort may deliver a novel obtainable, and cost-effective substitutional material to the costly concrete as shielding materials. The theoretical values of the mass attenuation coefficient were higher than the experimental values of the two clay compounds, R1 and R2, and these values increased when boron was added to them.

Conflict of interest

The authors declare no conflict of interest.

References

[1] S. A. Issa, "Effective atomic number and mass attenuation coefficient of PbO–BaO–B2O3 glass system," *Radiation Physics and Chemistry*, vol. 120, pp. 33-37, 2016.

[2] K. Kaur, K. Singh, and V. Anand, "Correlation of gamma-ray shielding and structural properties of PbO–BaO–P2O5 glass system," *Nuclear engineering and design*, vol. 285, pp. 31-38, 2015.

[3] Akram, M. Ali, Ahmed, Salih, "Influance Oof boron on gamma-ray shielding effecincy of clay material", *Journal of critical reviews*, vol. 7, no. 10, 2020.

[4] Aygün, B. "High alloyed new stainless steel shielding material for gamma and fast neutron radiation". *Nucl. Eng. Technol.* , vol. *52*, pp. 647–653, 2020.

[5] I. Akkurt and H. Canakci, "Radiation attenuation of boron-doped clay for 662, 1173 and 1332 keV gamma rays," *Iran. J. Radiat. Res.*, vol .9, no. 1, pp. 37-40: 2011.

[6] H. S. Mann, G. Brar, and G. Mudahar, "Gamma-ray shielding effectiveness of novel light-weight clay-flyash bricks," *Radiation Physics and Chemistry*, vol. 127, pp. 97-101, 2016.

[7] S. Tajudin, A. Sabri, M. A. Aziz, S. Olukotun, B. Ojo, and M. Fasasi, "Feasibility of clay-shielding material for low-energy photons (Gamma/X)," *Nuclear Engineering and Technology*, vol. 51, no. 6, pp. 1633-1637, 2019.

[8] J. H. Lambert, "Photometria sive de Mensura et gradibus Luminis," Nabu Press,2018 *Colorum et Umbrae, Eberhard Klett, Augsberg, Germany,* 1760.

[9] H. S. Mann, G. S. Brar, K. S. Mann, and G. S. Mudahar, "Experimental investigation of clay fly ash bricks for gamma-ray shielding," *Nuclear Engineering and Technology*, vol. 48, no. 5, pp. 1230-1236, 2016.

[10] J. M. Akande and S. A. Agbalajobi, "Analysis on some physical and chemical properties of Oreke dolomite deposit," *Journal of Minerals and Materials Characterization and Engineering*, vol. 01, no.02, pp.33-38, 2013.

[11] O. Içelli, K. S. Mann, Z. Yalçın, S. Orak, and V. Karakaya, "Investigation of shielding properties of some boron compounds," *Annals of Nuclear Energy,* vol. 55, pp. 341-350, 2013.

[12] E. Zorla, C. Ipbüker, A. Biland, M. Kiisk, S. Kovaljov, A. H. Tkaczyk, and V. Gulik , "Radiation shielding properties of high-performance concrete reinforced with basalt fibers infused with natural and enriched boron," *Nuclear engineering and Design,* vol. 313, pp. 306-318, 2017.

[13] S. Olukotun, S. Gbenu, F. Ibitoye, O. Oladejo, H. Shittu, M. Fasasi, F.A. Balogun , "Investigation of gamma radiation shielding capability of two clay materials," *Nuclear Engineering and Technology*, vol. 50, no. 6, pp. 957-962, 2018.